J. Ind. Geophys. Union ( July 2008 )
**Vol.12, No.3, pp.131-140**

# Estimation of land surface temperature over Delhi using Landsat-7 ETM+

**Javed Mallick, Yogesh Kant[1] and B.D.Bharath[1]**
GIS Department, STC-IT-CFS-GIS, Saudi Telecom, Saudi Arabia
[1]Indian Institute of Remote Sensing (NRSA), Dept. of Space, Govt. of India
4, Kalidas Road, Dehradun – 248 001
E.mail : ykanty@yahoo.com

**ABSTRACT**
Land surface temperature (LST) is important factor in global change studies, in estimating radiation budgets in heat balance studies and as a control for climate models. The knowledge of surface temperature is important to a range of issues and themes in earth sciences central to urban climatology, global environmental change, and human-environment interactions. In the study an attempt has been made to estimate surface temperature over Delhi area using Landsat-7 ETM+ satellite data. The variability of these retrieved LSTs has been investigated with respect to different land use / land cover (LU/LC) types determined from the Landsat visible and NIR channels. The classification uncertainties over different land use land cover were assessed and it has been observed that the classification uncertainties were found to be lowest using Minimum Noise Fraction (MNF) components. The emissivity per pixel is retrieved directly from satellite data and has been estimated as narrow band emissivity at the satellite sensor channel in order to have least error in the surface temperature estimation. Strong correlation is observed between surface temperature with Normalized Difference Vegetation Index (NDVI) over different LU/LC classes and the relationship is moderate with fractional vegetation cover (FVC). A regression relation between these parameters has also been estimated indicating that surface temperatures can be predicted if NDVI values are known. The results suggest that the methodology is feasible to estimate NDVI, surface emissivity and surface temperature with reasonable accuracy over heterogeneous urban areas.

## INTRODUCTION

The climate in and around cities and other built up areas is altered due to changes in LU/LC and anthropogenic activities of urbanization. The most imperative problem in urban areas is increasing surface temperature due to alteration and conversion of vegetated surfaces to impervious surfaces. These changes affect the absorption of solar radiation, surface temperature, evaporation rates, storage of heat, wind turbulence and can drastically alter the conditions of the near-surface atmosphere over the cities. The temperature difference between urban and rural settings is normally called urban heat island (UHI).

Land surface temperature can provide important information about the surface physical properties and climate which plays a role in many environmental processes (Dousset & Gourmelon 2003; Weng, Lu & Schubring 2004). Many studies have estimated the relative warmth of cities by measuring the air temperature, using land based observation stations. Some studies used measurements of temperature using temperature sensors mounted on car, along various routes (Yamashita 1996). This method can be both expensive and time consuming and lead to problems in spatial interpolation. Remote sensing might be a better alternative to the aforesaid methods. The advantages of using remotely sensed data are the availability of high resolution, consistent and repetitive coverage and capability of measurements of earth surface conditions (Owen, Carlson & Gillies 1998). In remote sensing, Thermal infrared (TIR) sensors can obtain quantitative information of surface temperature across the LU/LC categories. There are many available thermal infrared sensors to study LST. The Geostationary Operational Environmental Satellite (GOES) has a 4-km resolution in the thermal infrared, while the NOAA-Advanced Very High Resolution Radiometer (AVHRR), Terra and Aqua-Moderate Resolution Imaging Spectroradiometer (MODIS) have 1-km spatial resolution. High-resolution data from the Terra-Advanced Spaceborne Thermal Emission and Reflection Radiometer (ASTER) has a 90-m resolution and Landsat-7

Enhanced Thematic Mapper (ETM+) has a 60-m resolution in thermal region.

Land surface temperature is sensitive to vegetation and soil moisture, hence it can be used to detect land use/land cover changes, e.g. tendencies towards urbanization, desertification etc. Various studies have been carried out to investigate LST using the vegetation abundance (Weng, Lu & Schubring 2004). The major effects of the atmosphere are absorption, upward atmospheric emission, and the downward atmospheric irradiance reflected from the surface (Pierangelo et al., 2004). While the effects of aerosol absorption and scattering has not been considered in this study, good research has been carried out on the effects of these on radiances at infrared wavelengths and satellite derived land and sea surface temperatures (France & Cracknell 1994). The present study analyzes the potential of LST estimation using Landsat-7 ETM+ over heterogeneous urban area. For estimation of LST, derivation of surface emissivity is important. In many studies, the emissivity databases (Salisbury & D'Aria 1992, 1994) are used which are from laboratory measurements and do not represent the emissivity at the satellite pixel scale (60×60m of Landsat-7 in this case). Hence, the emissivity parameter per pixel needs to be estimated directly from satellite data to have an accurate estimation of LST. The study considers the spatial variations of LST over different LU/LC. The study also analyzes the relationship of vegetation density (NDVI) and FVC with LST.

## DESCRIPTION OF THE STUDY AREA

Delhi being a modern city with long history, with combination of different land use / land cover and vulnerable to atmosphere turbulence; hence has been chosen as the study area. It is geographically situated on latitude $28^0$ 23′ 17″ North – $28^0$ 53′ 00″ North and Longitude $76^0$ 50′ 24″ East – $77^0$ 20′ 37″ East and lies at an altitude between 213 and 305 meters and covering an area of 1,483 $km^2$. It is situated on the bank of river Yamuna (a tributary of the river Ganga). It is bordered in the east by the state of Uttar Pradesh and on the north, west, and south by the state of Haryana. Physically Delhi can be divided into three segments: the Yamuna flood plain, the ridge and the plain. The Yamuna flood plains are somewhat low-lying and sandy. The ridge constitutes the most dominating physiographic features of this territory. It originated from the Aravali hills of Rajasthan and entering Delhi from the south, extends in north-eastern direction. The ridge in Delhi which is predominately of thorny type forest (usually found in arid and semi arid zone). The extent of forest is around 111 $km^2$ 7.49 % of the total Delhi area). The rest of Delhi is categorized as a plain. The land use distribution in Delhi is described in Table 1.

**Table 1.** Land use distribution of Delhi

| Land use | Percentage of land |
|---|---|
| Residential | 45-55 |
| Commercial | 3-4 |
| Industrial | 4-5 |
| Green / Recreational | 15-20 |
| Public and Semi-Public Facilities | 8-10 |
| Circulation | 10-12 |

Source: Delhi Development Authority (DDA) Draft Master Plan, New Delhi

## SATELLITE DATA PROCESSING

Satellite dataset of Landsat-7 ETM+ over Delhi area of 22nd October, 1999 (day time, level-1G product, path/row 146/40) has been used in this study (cloud cover 0%).

DN values were converted to at-sensor radiance, for Landsat-7 ETM+ using

$$L_\lambda = Gain \times DN + Bias = \left( \frac{L_{\max} - L_{\min}}{255} \right) \times DN + Bias \quad ...(1)$$

where,

$L_\lambda$=spectral radiance at the sensor ($Wm^{-2}sr^{-1}\mu m^{-1}$)

Biss=$L_{\min}$

Landsat-7 ETM+ level-1G products were geometrically corrected data set. For standardization, Landsat -7 ETM+ Panchromatic data (15 m resolution) was compared with Aster 15 m data (VNIR) and was noticed that geometrical accuracy was low. Also the GPS readings from the ground did not match with these images. Hence there was a need to further rectify the dataset. The image was geometrically rectified to a common Universal Transverse Mercator (UTM) WGS84 coordinate system and were resampled to its spatial resolution using the nearest- neighborhood algorithm.

Considering the objectives and satellite data used, following LU/LC classification scheme has been adopted: high dense built-up, low dense built-up, commercial /industrial area, dense vegetation (forest), sparse vegetation (including parks), water bodies, fallow land, waste land/bare soil and agricultural cropland.

For image classification, a pre-field visit was done to have an idea of different LU/LC classes existing in the study area. Unsupervised classification was initially performed on Landsat-7 ETM+ for an idea

of the spectral separability of the land use/land cover classes. An extensive field survey was done with the priori knowledge using the unsupervised classification to identify sample points in the imagery for different LU/LC classes at various locations using GPS. Based on the collected sample sets for respective LU/LC classes, training sets were selected in the False Colour Composite (FCC) imagery for supervised classification using Maximum Likelihood Classification (MLC).

Minimum Noise Fraction (MNF) was performed on the Landsat-7 ETM+ data to reduce the data redundancy and correlation between spectral bands. MNF was applied to bands 1 to 7 (excluding band 6) on Landsat-7 ETM+ dataset. The first three MNF components of Landsat-7 ETM+ data was used to classify the image using the MLC while the other components were discarded due to the higher proportion of noise content.

## METHODOLOGY

At the pixel scale, natural surfaces are heterogeneous in terms of variation in emissivity. In addition, the emissivity is largely dependent on the surface roughness, nature of vegetation cover etc. In the present study an attempt has been made to derive emissivity by taking the fraction of vegetation cover per pixel in conjunction with NDVI. The fractional vegetation cover (FVC) for each pixel through satellite data is calculated using the following relation (Valor & Caselles 1996),

$$P_V = \frac{\left(1 - i/i_g\right)}{\left(1 - i/i_g\right) - k\left(1 - i/i_v\right)} \quad ...(2)$$

where,
$i_g$= NDVI value of pure soil pixel
$i_v$= NDVI value of pure vegetation pixel
$k=(\rho_{2v}-\rho_{1v})/(\rho_{2g}-\rho_{1g})$
where $\rho_{2v}$, $\rho_{1v}$ are reflectance in the NIR and red region for pure vegetation pixels; $\rho_{2g}$ and $\rho_{1g}$ are the reflectance in the NIR and red region for pure soil pixels respectively, and '*i*' is the NDVI value of mixed pixels. The application of the model has two parts. For the first part, the vegetation and bare soil proportions are obtained from the NDVI of pure pixels.

Surface emissivity on pixel scale is derived using NDVI in conjunction with proportional vegetation cover (Valor and Caselles 1996).

$$\varepsilon=\varepsilon_v P_v+\varepsilon_s(1-P_v)+d\varepsilon \quad ...(3)$$

where

$$d\varepsilon=4\langle d\varepsilon\rangle P_v(1-P_v) \quad ...(4)$$

where,
$P_v$ is the vegetation cover fraction, $(1-P_v)$ the soil cover fraction, $\varepsilon_v$ is the vegetation canopy emissivity, $\varepsilon_s$ is the bare soil emissivity. The term error in emissivity value, $\langle d\varepsilon\rangle$ (Valor & Caselles 1996; Caselles & Sobrino 1989) is the mean weighted value that takes into account the mean of emissivity value of different surface types. Weighted value $(d\varepsilon)$ of 0.04 (approximation) has been adopted in the present study. For the calculation of emissivity values the term $\varepsilon_v$ and $\varepsilon_s$, i.e., the emissivity values of pure vegetation and soil pixels are taken as 0.978 and 0.914 respectively from literature.

NDVI is estimated using proportion vegetation cover

$$NDVI=i_v P_v+i_s(1-P_v)+di \quad ...(5)$$

where, $i_v$ is the pure vegetation NDVI, $i_s$ is the pure soil NDVI in the study area and *di* is the error in NDVI. The proportion of vegetation cover for each pixel through satellite data is calculated using the relation (2).

Surface emissivity is estimated using the relation,

$$\varepsilon_{(8-14)} = \frac{\varepsilon_v - \varepsilon_s}{i_v - i_s} NDVI + \frac{\varepsilon_s(i_v + di) - \varepsilon_v(i_s + di)}{i_v - i_s} + d\varepsilon \quad ...(6)$$

This approach requires preliminary knowledge of vegetation and bare soil NDVI, vegetation and bare soil emissivities and the shape factors.

The narrow-band emissivity ($\varepsilon_i$) at the sensor resolution is calculated from the correlation between broad band ($\varepsilon_{8\text{-}14}$) (Rubio, Caselles & Badenas 1997)

$$\varepsilon_i = a\ \varepsilon_{8\text{-}14} + b \quad ...(7)$$

where, i = band 6 of Landsat-7, 'a' corresponds to gain and 'b' for intercept.

Band 6L was used in the estimation of surface temperature. The thermal radiance values were converted to surface temperatures using the pre-launch calibration constants (Schott & Volchok 1985). The surface temperature for Landsat-7 ETM+ is estimated using,

$$Ts_6 = \frac{K_2}{Ln\ [\varepsilon_i\ x\ K_1 / L_\lambda + 1]}$$

where $Ts_6$ is the effective satellite temperature (Kelvin), $K_2$ and $K_1$ are calibration constants and $L_\lambda$ is spectral radiance in $Wm^{-2}sr^{-1}\mu m^{-1}$.

## RESULTS

### Analysis of Land use/Land cover :

The FCC image of Landsat-7 ETM+ data (22nd October, 1999) covered approximately 99% of the study area is shown in Fig. 1 (extreme western portion of

the image is not covered in the satellite pass). Maximum Likelihood classification (MLC) was applied on the original bands of Landsat-7 ETM+ image. From the classified image it is observed that most of the agricultural cropland is classified as sparse vegetation due to similar spectral reflectance characteristics. It is also observed that some of the sparse vegetation is getting mixed with low dense built-up and fallow land is getting mixed with waste land/bare soil. The user's accuracy is lower in case of commercial /industrial area (57.06%), followed by sparse vegetation (65.06%) and dense vegetation (77.99%). The highest user's accuracy is found in water bodies (92.67%), followed by fallow land (89.65%) and low dense built-up (89.44%). The overall classification accuracy of 79.90% and kappa statistics of 0.7562 has been observed.

It is observed that the classification results improved using the MNF components. The highest user's accuracy is found in water bodies (99.70%), followed by fallow land (94.18%), agricultural cropland (90.59%), and low dense built-up (90.35%). Lower user's accuracy is found over commercial/industrial areas (60.43%). Analysing the classification results, improvement in user's accuracy is observed over sparse vegetation (7.63% higher), followed by water bodies (7.03% higher) and agricultural cropland (6.48% higher) compared to classification (MLC) using original bands. Less improvement in user's accuracy is found in low dense built-up area (0.91% higher) compared to conventional classification of original bands using MLC. An overall improved classification accuracy of 82.75% and kappa statistics of 0.7903 is observed. The classified image with original bands showed low accuracy due to the fact that there are regions of spectral overlapping of features. It is observed that Maximum Likelihood classification with MNF components significantly increases the user's accuracy over sparse vegetation, dense vegetation, agricultural cropland and waste land/bare soil. This is mainly attributed to the reduction in noise and decrease in spectral correlation between bands.

**Analysis of vegetation density (NDVI) using Landsat -7 ETM+ :**

Figure 2 (A) shows the spatial distribution of NDVI from the Landsat image. The NDVI values estimated

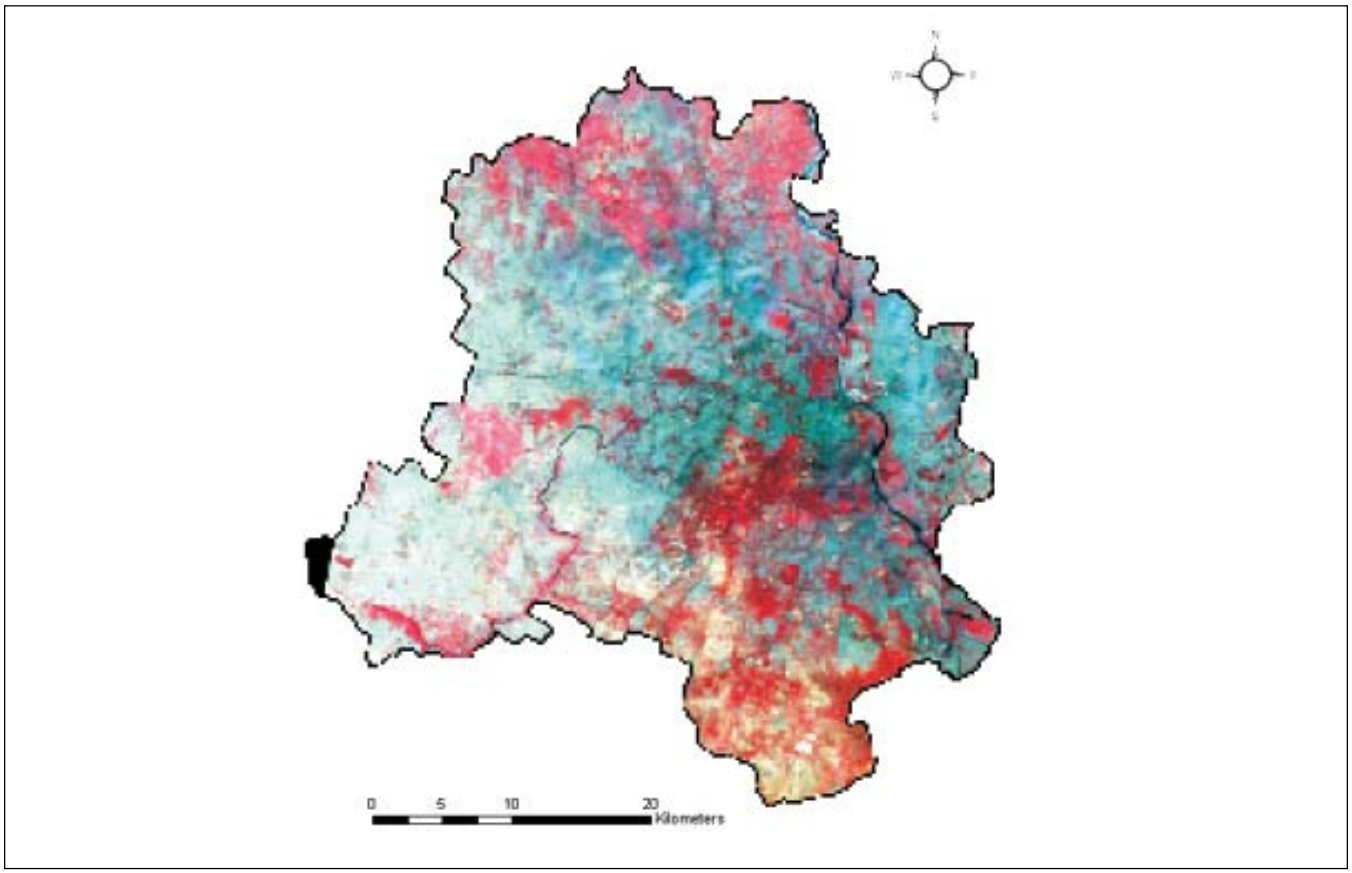


**Figure 1.** False Colour Composite (FCC) (Bands 2, 3 and 4) image of Landsat-7 ETM+ data of Delhi.

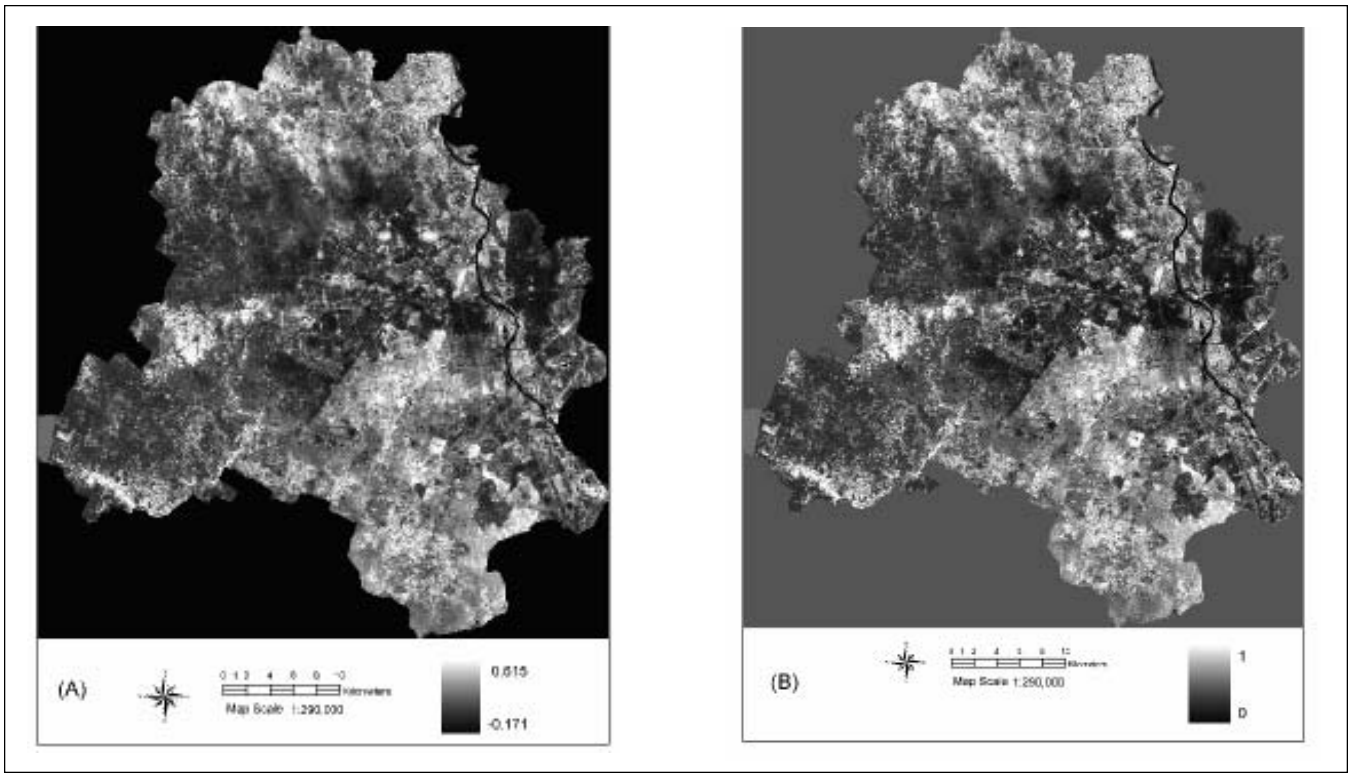


**Figure 2.** Spatial distribution of (A) NDVI and (B) Fractional vegetation cover from Landsat-7 ETM+.

are in the range of -0.171 to 0.615, having a mean value of 0.183 with standard deviation of 0.086. It is seen that lower NDVI value (dark area) corresponds to high dense built-up area on the eastern side of river Yamuna, CBD (central business district) of Delhi and old Delhi on the northern side of CBD. Higher NDVI values (bright areas) are observed in the central ridge (forest), north-west and south-west part of image. Medium NDVI values (grey areas to bright areas) are observed over agricultural croplands, in the northern part of the image. A similar distribution of vegetation is found in the FVC image [Fig.2(B)]), which is represented in range from 0 to 1 having a mean value of 0.206 with standard deviation of 0.0698. It is observed that the dense vegetation (forest), sparse vegetation (grass/park) and agricultural cropland appears in bright tone, while waste land/bare soil appears in bright to gray tone. Residential (low and high dense built-up areas) and water bodies appear in dark tone. The lowest fractional vegetation value is over water bodies with the mean value of 0.054 (ranging from 0.014 to 0.099) and corresponding mean NDVI value of -0.038 (ranging from -0.127 to 0.119). Analysis between the NDVI and the FVC image shows a positive Pearson's correlation coefficient of 0.753 and correlation is significant at the level of 0.01 (1-tailed).

These differences indicate not only distinct computation procedures for deriving NDVI and FVC, but also their relationship to their vegetation density/ vegetation abundance. It is also observed that the relationship between these two vegetation indicators is not linear for different land use/land cover categories. These results are further analyzed with surface temperature.

From the derived emissivty values, the maximum values are observed over agricultural cropland that ranges from 0.964 to 0.975 (mean of 0.970 and standard deviation of 0.0018). Paddy is mainly grown in the agricultural belt of the region with patches of horticulture (mainly seasonal vegetables). The paddy during October month was in the growing stage hence, most of the field had full extent of paddy with minimum of the soil background. Dense vegetation (mainly forest) depicted emissivity values in the range 0.955 to 0.970 (mean of 0.961 and standard deviation of 0.001) as the vegetation in forest area is of shrubs type (water has the highest emissivity value). The emissivity values over the sparse vegetation category (mainly parks, playground etc.) are found to be in the range of 0.949 to 0.957 (mean of 0.953 and standard deviation of 0.002). The values over low dense built-up, high dense built-up and commercial/ industrial are difficult to segregate as they are very much overlapping. Hence, they are merged under urban

(concrete), as basically concrete structures are common in these categories. The emissivity value over urban (concrete) varies from 0.890 to 0.935 (mean 0.912 to and standard deviation of 0.012). The values over waste land/bare soil found to vary from 0.880 to 0.915 (mean 0.896 and standard deviation of 0.02). River Yamuna flows from north-east to south-east of the study area. When the river enters the central part of the city it is being polluted by industrial sewage, anthropogenic wastes and activities. This is also reflected in the NDVI and emissivity values over the turbid water. The emissivity values over such part of turbid water area are from 0.890 to 0.910. The clear water bodies are found in the northern area and some portions of river Yamuna towards the boundary of the study area. The emissivity values over clear water bodies are found to be around 0.989. The derived emisssivity values over different features have been compared with those in the literature (Salisbury & D'Aria 1992; Rubio, Casellas & Badenas 1997; Van de Griend & Owe 1993) and found to be in agreement (error of around 1-2%). Table 2 shows the comparison of the estimated parameters by taking few samples of pure pixels in respective categories with their mean. The values of NDVI, FVC for features may be higher in this table as they are mean of few pure samples taken for the purpose, but the trend between features is followed.

**Analysis of surface temperature of LANDSAT-7 ETM+ :**

Figure 3 shows the spatial distribution of surface temperature of Landsat-7 ETM+. The LST ranged from 22.89 to 46.01 °C (mean of 34.56°C and standard deviation of $3.383^0$ C). It is observed from the image that west and south-west part exhibits high temperature mainly due to waste land/bare soil and fallow land. Some of the high temperature zones are also seen in the central part of the image mainly due to commercial/industrial land use.

Table 3 shows the estimated surface temperature values over different LU/LC classes. The values are maximum for fallow land ranging from 40.08 to 45.17 °C (mean of 42.88°C) and minimum over water bodies ranging from 23.92 to 32.93°C (mean of 26.54°C). Commercial/industrial land use surface temperature ranges from 33.01 to 40.90°C (mean value 36.48 °C). The impact of vegetation is clearly seen as low temperature values are observed over agricultural cropland, dense vegetation (forest), sparse vegetation (grass/park) land use categories.

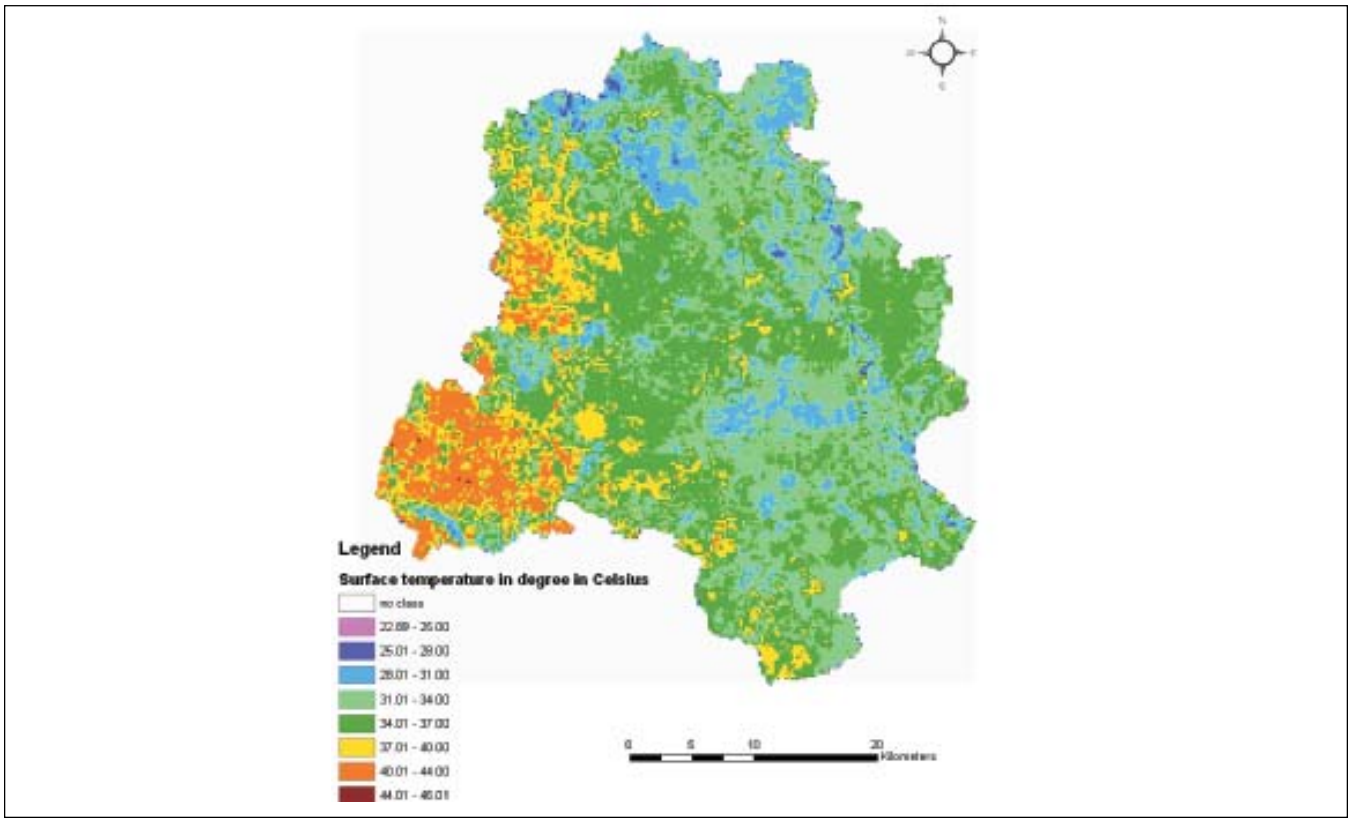


**Figure 3.** Spatial distribution of land surface temperature over the study area using Landsat-7 ETM+.

**Table 2.** Estimated parameters from Landsat -7 ETM+.

| Sl. No. | Features | Fractional Vegetation cover | NDVI | Emissivity |
|---|---|---|---|---|
| 1. | Water bodies | 0.000 | -0.070 | 0.989 |
| 2. | Agricultural cropland | 0.977 | 0.472 | 0.972 |
| 3. | Dense vegetation (forest) | 0.682 | 0.377 | 0.967 |
| 4. | Sparse Vegetation (Grass) | 0.507 | 0.320 | 0.957 |
| 5. | Urban (built-up) | 0.154 | 0.107 | 0.912 |
| 6. | Waste land/bare soil | 0.030 | 0.027 | 0.896 |

**Table 3.** Statistics of surface temperature over different land use/ land cover categories.

| Land use / land cover | Min. temp (°C) | Max. temp (°C) | Mean (°C) | Standard Deviation (SD) |
|---|---|---|---|---|
| Water bodies | 23.92 | 32.93 | 26.54 | 1.702 |
| Agricultural cropland | 27.01 | 30.78 | 28.49 | 0.820 |
| Dense vegetation | 27.33 | 31.95 | 29.22 | 0.915 |
| Sparse vegetation | 29.01 | 33.98 | 30.85 | 1.233 |
| Low dense built-up | 29.01 | 35.96 | 33.14 | 1.707 |
| High dense built-up | 34.04 | 37.64 | 35.55 | 0.527 |
| Commercial/industrial | 33.01 | 40.90 | 36.48 | 1.901 |
| Waste land/bare soil | 35.06 | 44.42 | 39.18 | 1.021 |
| Fallow land | 40.08 | 45.17 | 42.88 | 0.834 |

**Table 4.** Comparison of satellite derived day time surface temperature with field measured values.

| Features | Field observation during 19th to 24th Oct 2005 (10.30 to 12.00 local time) in °C | Landsat-7 ETM+ of 22nd Oct, 1999 in °C | UTM Coordinates (meter) |
|---|---|---|---|
| Vegetation | 33.20 | 30.15 | 711600 / 3168804 |
| Vegetation | 34.50 | 31.18 | 713443 / 3166854 |
| Vegetation | 34.25 | 31.16 | 715177 / 3164361 |
| Vegetation | 36.50 | 32.37 | 718428 / 3167288 |
| **Average** | 34.61 | 31.21 | - |
| Bare soil | 48.25 | 43.25 | 693503 / 3158835 |
| Bare soil | 47.16 | 43.11 | 693620 / 3159300 |
| Bare soil | 47.62 | 43.19 | 683740 / 3067862 |
| Bare soil | 47.06 | 43.47 | 691421 / 3174336 |
| **Average** | 47.45 | 43.20 | - |
| Concrete (Urban) | 34.80 | 35.41 | 723630 / 3174656 |
| Concrete (Urban) | 34.60 | 36.84 | 717275 / 3169419 |
| Concrete (Urban) | 35.12 | 36.93 | 719368 / 3182416 |
| Concrete (Urban) | 34.62 | 36.74 | 725432 / 3134986 |
| Concrete (Urban) | 34.41 | 36.76 | 713265 / 3166231 |
| **Average** | 34.71 | 36.54 | - |

As the date of satellite data being 22nd October 1999, field measurements are not available during this period. For comparison purpose the field measurements were taken in October 2005 keeping the time and same period of season. In order to compare the estimated surface temperature values from satellite data with the field measurements, a field campaign from October 19 to October 24, 2005 was carried out and measurements were taken over different LU/LC features (the same LU/LC were there in 1999). Table 4 shows the comparison between the satellite derived surface temperature values with that of field measured and is inferred that the retrieved values are in good agreement with an error of around 4 $^0$C.

**Relationship between vegetation density and surface temperature :**

Table 5 shows the correlation (surface temperature with NDVI and FVC) for different land use/land cover categories. It is inferred that NDVI and FVC values tend to be negatively correlated with the surface temperature (with the exception of water). The strongest negative correlation between surface temperature and NDVI values is found over dense vegetation (-0.752) followed sparse vegetation (-0.709), agricultural cropland (-0.687), commercial/industrial land use (-0.626). The strongest, negative correlation between surface temperature and FVC values is found over dense vegetation (-0.493) followed sparse vegetation (-0.439), agricultural cropland (-0.437) and waste land/bare soil (-0.416). Least correlation is found over high dense built-up (-0.316).

Strong correlation between surface temperatures with NDVI is observed over dense vegetation, sparse vegetation and agricultural cropland, which assures a potential of using linear regression to predict surface temperatures if NDVI values are known whereas correlation with FVC is moderately observed over dense vegetation, sparse vegetation and agricultural cropland. Hence surface temperature can be predicted with reasonable accuracy using NDVI.

Table 6 shows the regression coefficient between surface temperature with NDVI and FVC for dense vegetation, sparse vegetation and agricultural cropland with significance levels of 0.01 levels. Coefficient of determination ($R^2$) for NDVI over dense vegetation is highest (0.566), followed by sparse vegetation (0.502) and agricultural cropland (0.400). It is observed that coefficient of determination ($R^2$) of surface temperature with NDVI is better as compared with that for FVC.

**Table 5.** Correlation coefficient between Surface temperature with NDVI and FVC over different land use/land covers categories.

| Land use/land cover | Number of sample pixels | Correlation (ST versus NDVI) | Correlation (ST versus FVC) |
|---|---|---|---|
| Agricultural cropland | 897 | -0.687 | -0.437 |
| Dense vegetation (forest) | 1006 | -0.752 | -0.493 |
| Sparse vegetation (Grass/park) | 919 | -0.709 | -0.439 |
| Low dense built-up | 891 | -0.623 | -0.318 |
| High dense built-up | 963 | -0.394 | -0.316 |
| Commercial/industrial | 926 | -0.626 | -0.406 |
| Waste land/bare soil | 1026 | -0.599 | -0.416 |
| Water bodies | 644 | 0.035 | 0.027 |

**Table 6.** Linear regression for predicting surface temperature over land use/land cover classes.

| Land use /land cover | Linear regression (NDVI) | Linear regression (FVC) | Coefficient of determination (NDVI), $R^2$ | Coefficient of determination (FVC), $R^2$ |
|---|---|---|---|---|
| Dense vegetation (forest) | Y = (-28.557) $X_{NDVI}$ + 39.488 | Y = (-18.170) $X_{FVC}$ + 35.286 | 0.566 | 0.243 |
| Sparse vegetation (grass /park) | Y = (-37.101) $X_{NDVI}$ + 41.804 | Y = (-16.079) $X_{FVC}$ + 34.879 | 0.502 | 0.191 |
| Agricultural cropland | Y = (-26.154) $X_{NDVI}$ + 38.794 | Y = (-11.429) $X_{FVC}$ + 33.921 | 0.400 | 0.193 |

## CONCLUSIONS

In the research the potential of remote sensing to study the urban morphology is presented by estimating the spatial distribution and intensities of geo-physical parameters. Emissivity and surface temperature enables in better understanding of the overall urban land classes and in turn helps in understanding the energy budget issues. This provides causes and effects, as an important addition to conventional methods of monitoring the urban environment. The estimated emissivity values over few land use/land cover of Landsat-7 ETM+ have been compared with the literature values. The results show that the satellite derived emissivity values are in the acceptable range and the NDVI and fractional vegetation cover are effective in deriving surface emissivity. The derived surface temperature values are found to be in good agreement with the field measured values, indicating that the methodology can be adopted for the study over urban areas.

## ACKNOWLEDGEMENTS

The authors acknowledge their sincere gratitude to Director, NRSA and Dean, IIRS for the constant encouragement and useful suggestions during the course of the study.

## REFERENCES

Caselles, V. & Sobrino, J.A., 1989. Determination of frosts in orange groves from NOAA-9 AVHRR data. Remote Sensing of Environment, 29, 135-146.

Dousset, B. & Gourmelon, F., 2003. Satellite multi-sensor data analysis of urban surface temperatures and landcover, ISPRS Journal of Photogrammetry and Remote Sensing. 58, (1-2), 43-54.

France, G.B. & Cracknell, A.P., 1994. Retrieval of land and sea surface temperature using NOAA-11 AVHRR data in north-eastern Brazil, International Journal of Remote Sensing, 15, 1695-1712.

Owen, T.W., Carlson, T.N. & Gillies, R.R., 1998. Remotely sensed surface parameters governing urban climate change, Internal Journal of Remote Sensing, 19, 1663-1681.

Pierangelo, C., Ch'edin, C., Jacquinet-Husson, N. & Armante, R., 2004. Dust altitude and infrared optical depth from ARIS, Atmospheric Chemistry and Physics Discussions, 4, 333-3358.

Rubio, E., Caselles, V. & Badenas, C., 1997. Emissivity measurements of several soils and vegetation types in the 8-14$\mu$m wave band: Analysis of two field methods, Remote Sensing of Environment, 59, 490-521.

Salisbury, J.W. & D'Aria, D.M., 1992. Emissivity of Terrestrial Materials in the 8 to 14micro meter Atmospheric Window, Remote Sensing Environment, 42, 83-106.

Salisbury, J.W. & D'Aria, D.M., 1994. Emissivity of Terrestrial Materials in the 2 to 5micro meter Atmospheric Window, Remote Sensing Environment, 47 (3), 345-361.

Schott, J.R. & Volchok, W.J., 1985. Thematic mapper thermal infrared calibration, Photogrammetric Engineering and Remote Sensing, 51, 1351-1357.

Valor, E. & Caselles, V., 1996. Mapping land surface emissivity from NDVI. Application to European, African and South American areas, Remote Sensing of Environment, 57, 167-184.

Van de Griend, A.A. & Owe, M., 1993. On the relationship between thermal emissivity and the normalized difference vegetation index for natural surfaces, International Journal of Remote Sensing, 14, 1119-1131.

Weng, Q., Lu, D. & Schubring, J., 2004. Estimation of land surface temperature-vegetation abundance relationship for urban heat island studies, Remote Sensing of Environment, 89(4), 467-483.

Yamashita., 1996. Detail Structure of Heat Island Phenomena from Moving Observations from Electric Trans Cars in Metropolitan Tokyo, Atmospheric Environment, 30, 429 435.

(Accepted 2008 May 26. Revised received 2008 May 19; in original form 2008 February 27)

**Mr. Javed Mallick** obtained his Masters of Science degree in Geography from Jamia Millia Islamia, India in 2001. In the year 2005, he obtained Master's degree with specialization in Geoinformatics from Geoinformation Science and Earth Observation (ITC), The Netherlands. He has worked as a Research Associate with TERI (The Energy and Resources Institute), New Delhi, till 2007. Presently, he is working as a GIS Specialist with Saudi Telecom, Kingdom of Saudi Arabia. His research areas are image processing, geospatial and geostatistical analysis and geodatabase, Digital Elevation Models. Digital Photogrammetry expertise includes Stereo Compilation, Terrain extraction, Orthophoto and Mosaic Generation, Feature extraction, editing and Image corrections.

**Dr. Yogesh Kant** obtained his Master of Science degree in Physics from HNB Garhwal University in 1995 and subsequently Ph.D in Physics from Osmania University, Hyderabad in 2000. Presently, he is working as Scientist in Indian Institute of Remote Sensing (NRSA), Dehradun. His research field pertains to Remote sensing application to land surface processes, environmental physics. He has developed algorithms for extraction of geo-physical parameters using satellite data, participated in BIBEX, INDOEX field campaigns related to gas emission and aerosols and has experience in collecting data from ground based instruments. Published over 40 research papers in various National and International Journals, he was conferred IGBP START Young Scientist award in the year 2002. He is a member of IGU, ISRS and visited Japan, Syria, The Netherlands for presenting his research works.

**Mr. B.D. Bharath** holds Bachelor degree in Architecture, Masters in City Planning (MCP) from IIT Kharagpur in 1997. Presently, he is working as Scientist in Human Settlement Analysis Division, Indian Institute of Remote Sensing (NRSA), Dehradun. His research field pertains to Remote Sensing application to urban planning. He is a member of Institute of Town Planners (India) and Indian Society of Remote Sensing.